

Carbon Dioxide: A Waste Product in the Catalytic Cycle of α -Ketoglutarate Dependent Halogenases Prevents the Formation of Hydroxylated By-Products

Sam P. de Visser^{*,†} and Reza Latifi[‡]

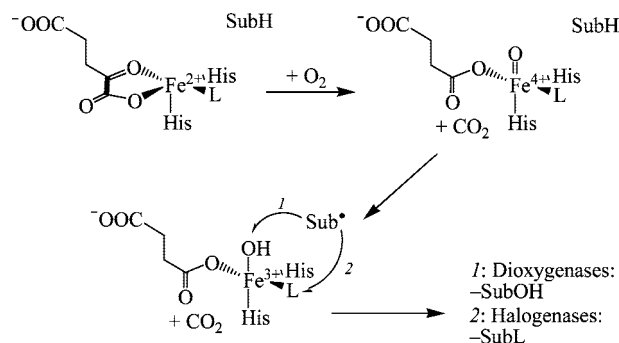
Manchester Interdisciplinary Biocenter and the School of Chemical Engineering and Analytical Science, The University of Manchester, 131 Princess Street, Manchester M1 7DN, United Kingdom, and Chemistry Department, Sharif University of Technology, P.O. Box 11155-3615, Tehran, Iran

Received: November 5, 2008

We present the first density functional theory study on α -ketoglutarate dependent halogenases and focus on the mechanism starting from the iron(IV)-oxo species. The studies show that the high-valent iron(IV)-oxo species reacts with substrates via an initial and rate determining hydrogen abstraction that is characterized by a large kinetic isotope effect (KIE) of 26.7 leading to a radical intermediate. This KIE value is in good agreement with experimental data. The reaction proceeds via two-state reactivity patterns on competing quintet and septet spin state surfaces with close lying hydrogen abstraction barriers. However, the septet spin radical intermediate gives very high barriers for hydroxylation and chlorination whereas the barriers on the quintet spin state surface are much lower. The calculations give extra information regarding the nature of the intermediates and a prediction of a new low-energy mechanism starting from the radical intermediate, whereby a waste product from an earlier step in the catalytic cycle (CO_2) is recycled and takes the hydroxyl radical away to form bicarbonate via an OH trapping mechanism. As a consequence, this mechanism prevents the occurrence of hydroxylated byproduct and gives a rationale for the sole observance of halogenated products. By contrast, a direct halogenation reaction cannot compete with hydroxylation due to higher reaction barriers. Our findings support experimental work in the field and give a rationale for the lack of hydroxylation products in α -ketoglutarate dependent halogenases.

Many biological systems utilize molecular oxygen on an iron center for, for example, substrate monooxygenation, dioxygenation, as well as halogenation.¹ The α -ketoglutarate dependent dioxygenases are a broad range of enzymes involved in the biosynthesis of collagen in mammals, DNA and RNA base repair, and the biosynthesis of antibiotics in microbes.^{1,2} These enzymes typically contain a mononuclear nonheme iron center that is bound to two histidine and one aspartic acid residue via a 2His/1Asp structural motif.^{1,2} Spectroscopic studies characterized the active species as an iron(IV)-oxo oxidant that reacts with substrates with a large kinetic isotope effect.^{3,4} A closely related group of enzymes are the α -ketoglutarate dependent halogenases (α KDH) that are involved in the production of halogenated compounds, as appear, for example, in the biosynthesis of vancomycin and chlortetracycline.⁵ The α KDH have a similar active site structure to the α -ketoglutarate dependent dioxygenases, such as taurine/ α -ketoglutarate dioxygenase (TauD), but contain a 2His/1L (L = halogen) motif. Nevertheless, the catalytic cycle of α KDH closely resembles that of the TauD, whereby α -ketoglutarate, substrate, and molecular oxygen bind to an iron center. Subsequently, one oxygen atom of O_2 is donated to α -ketoglutarate to form succinate, CO_2 and a high-valent iron(IV)-oxo complex (Scheme 1). It has been proposed that after the hydrogen abstraction the halide is abstracted by

SCHEME 1: Catalytic Cycle of α -Ketoglutarate Dependent Halogenases and Dioxygenases



the substrate rest-group to give halogenated products, but this hypothesis was disputed by recent density functional theory (DFT) studies on a biomimetic model complex that showed a preference of regioselective hydroxylation over chlorination.⁶ The question is therefore how these enzymes avoid generating hydroxylated byproduct. To resolve this tantalizing problem and to gain insight into how α KDH utilize molecular oxygen on an iron center to give chlorinated products, we set up a model of their active site and studied the competitive hydroxylation versus chlorination of a model substrate.

The model of the active site of α KDH is based on that for TauD⁷ and contains an iron(IV)-oxo group linked to two imidazole groups (mimicking the two histidine ligands), a

* To whom correspondence should be addressed. E-mail: sam.devisser@manchester.ac.uk.

[†] The University of Manchester.

[‡] Sharif University of Technology.

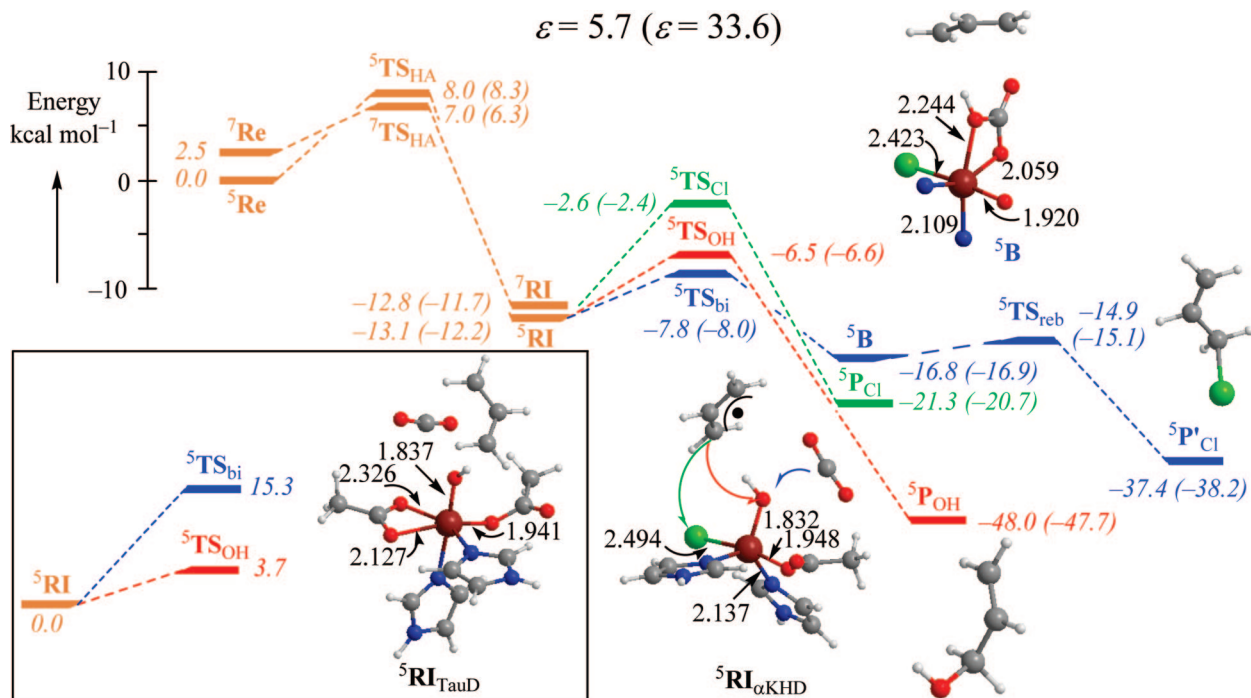


Figure 1. Potential energy landscape of competitive hydroxylation and halogenation reactions of propene by the iron(IV)-oxo species (^5Re) of α -ketoglutarate dependent halogenase. All energies are in kcal mol^{-1} relative to ^5Re calculated with UB3LYP/B1 and contain zero-point and solvation corrections. Extracts of optimized geometries contain bond lengths in angstroms. The three possible reaction mechanisms starting from ^5RI are shown in green (direct chlorination), red (hydroxylation), and blue (OH trapping). The competitive hydroxylation and OH trapping mechanisms for TauD are shown in the box.

chloride anion, α -ketopropionate (for α -ketoglutarate), carbon dioxide, and substrate (propene). All calculations were performed using the UB3LYP hybrid density functional method as implemented in *Jaguar* 7.0.⁸ We used a double- ζ quality LACVP basis set on iron that contains a core potential and 6-31G on the rest of the atoms (basis set B1) for optimizations and frequencies.⁹ Subsequent, single point calculations with a triple- ζ quality LACV3P+ basis set on iron in combination with 6-311+G* on the rest of the atoms confirmed the energetics. The effect of the environment on the ordering and relative energies of the reaction barriers was tested with the addition of a dielectric constant of magnitude $\epsilon = 5.7$ or 33.62 in *Jaguar*. Recent studies on a series of hydrogen abstraction reactions of substrates by the iron(IV)-oxo active species of cytochrome P450 enzymes showed that relative barrier heights can be calculated using these methods with a standard deviation of about 1–2 kcal mol^{-1} .¹⁰ Therefore, relative barrier heights of about 2 kcal mol^{-1} should distinguish between different reaction mechanisms accurately.

Figure 1 shows the potential energy landscape of competitive chlorination and hydroxylation of propene by our αKDH model as calculated with DFT. The reactant species is an iron(IV)-oxo (labeled ^5Re) with a quintet spin ground-state that is well separated from the septet, triplet and singlet spin states in $\epsilon = 5.7$ (by 2.5, 9.1, and 18.1 kcal mol^{-1} , respectively); the spin state ordering is similar to that obtained for TauD models.⁷ The reaction starts with a hydrogen atom abstraction from the substrate via a barrier TS_{HA} to form a radical intermediate (RI). The barriers on the septet and quintet spin state surfaces are close in energy, but the septet spin state surface encounters high barriers for the subsequent steps in the reaction mechanism (Supporting Information), therefore, products are only formed on the quintet spin state surface. The rate determining step in the reaction mechanism is via $^5\text{TS}_{\text{HA}}$ and substitution of the hydrogen atoms of the substrate by deuterium gives a

kinetic isotope effect (KIE) of 26.7 with tunneling corrections included, in excellent agreement with experimentally determined KIE values.⁴ The barrier $^5\text{TS}_{\text{HA}}$ is 8.0 kcal mol^{-1} in a dielectric constant of $\epsilon = 5.7$, which is slightly higher in energy than that calculated for TauD using a similar model and the same methods.⁷ Therefore, the substitution of a carboxylic acid group of an aspartate residue by a chloride anion induces a destabilizing effect on the hydrogen abstraction reaction and raises it by a couple of kcal mol^{-1} . The radical intermediate (^5RI) can transfer the chloride atom to the allyl radical via a barrier $^5\text{TS}_{\text{Cl}}$ to form the chlorinated product ($^5\text{P}_{\text{Cl}}$) or rebound the hydroxyl group via a barrier $^5\text{TS}_{\text{OH}}$ to form hydroxylated products ($^5\text{P}_{\text{OH}}$). Thus, similarly to the studies of Noack and Siegbahn on a different biomimetic system, the direct chlorination reaction is higher in energy than the hydroxylation reaction so that dominant hydroxylation products would be expected, which is in disagreement with experiment. An alternative mechanism is shown in blue in Figure 1, whereby carbon dioxide byproduct from an earlier step in the catalytic cycle attacks the hydroxyl group in ^5RI to form a bicarbonate complex (^5B) via a barrier $^5\text{TS}_{\text{bi}}$. A subsequent chlorination reaction via $^5\text{TS}_{\text{reb}}$ gives chlorinated products ($^5\text{P}'_{\text{Cl}}$). As follows from Figure 1, this is a low-energy alternative that leads to chlorinated products by shuttling the hydroxyl group away from the reaction center and thereby preventing the formation of hydroxylated products. This is an essential reaction in αKDH enzymes because of the large exothermicity of the hydroxylation reaction. Although the OH trapping mechanism is entropically disfavored with respect to the hydroxylation reaction, even at the free energy scale it is the expected dominant reaction mechanism. Nevertheless, the formation of ^5B from ^5RI is thermoneutral at the free energy scale in a dielectric constant of $\epsilon = 33.6$.

To ascertain that the OH trapping mechanism is unfeasible in hydroxylases, such as TauD, we calculated this mechanism for a TauD model (shown in the box in Figure 1). Thus, since

the carboxylic acid group of Asp₁₀₁ binds to the metal as a bidentate ligand in TauD, the metal in the hydroxo-iron complex ($^5\text{RI}_{\text{TauD}}$) is hexa-coordinated, whereas it is pentacoordinated in the hydroxo-iron complex of αKHD ($^5\text{RI}_{\alpha\text{KHD}}$). Thus, in the pentacoordinated system, the chloride and acetic acid groups bend away and make space for the incoming CO₂ molecule thereby lowering the OH trapping barrier. By contrast, the repulsive interactions of CO₂ with the anionic ligands in $^5\text{RI}_{\text{TauD}}$ raise the OH trapping barrier and lead to dominant hydroxylated products.

In summary, DFT calculations on the chlorination reaction of substrates by αKHD predict a novel mechanism whereby hydroxylated products are avoided. The reaction starts from the iron(IV)-oxo active species that abstracts a hydrogen atom from the substrate via a rate determining transition state and with an elevated KIE value in agreement with experimental studies. The hydroxo-iron complex reacts with CO₂ products from an earlier step in the catalytic cycle that shuttles the hydroxo group away by forming bicarbonate and thereby preventing the occurrence of hydroxylated byproduct. This mechanism supports experimental studies in the field and gives a rationale for the lack of hydroxylated byproduct in the reaction mechanism of halogenases.

Acknowledgment. The National Service of Computational Chemistry Software (NSCCS) is acknowledged for providing CPU time.

Supporting Information Available: Tables with group spin densities, charges and absolute energies, Figures with optimized geometries, and geometry scans, Cartesian coordinates of all

structures described in this work, and detailed methods. This material is available free of charge via the Internet at <http://pubs.acs.org>.

References and Notes

- (1) (a) Solomon, E. I.; Brunold, T. C.; Davis, M. I.; Kemsley, J. N.; Lee, S.-K.; Lehnert, N.; Neese, F.; Skulan, A. J.; Yang, Y.-S.; Zhou, J. *Chem. Rev.* **2000**, *100*, 235–349. (b) Costas, M.; Mehn, M. P.; Jensen, M. P.; Que, L., Jr. *Chem. Rev.* **2004**, *104*, 939–986.
- (2) (a) Ryle, M. J.; Hausinger, R. P. *Curr. Opin. Chem. Biol.* **2002**, *6*, 193–201. (b) Bollinger, J. M., Jr.; Price, J. C.; Hoffart, L. M.; Barr, E. W.; Krebs, C. *Eur. J. Inorg. Chem.* **2005**, 4245–4254. (c) Abu-Omar, M. M.; Loaiza, A.; Hontzas, N. *Chem. Rev.* **2005**, *105*, 2227–2252.
- (3) (a) Proshlyakov, D. A.; Henshaw, T. F.; Monterosso, G. R.; Ryle, M. J.; Hausinger, R. P. *J. Am. Chem. Soc.* **2004**, *126*, 1022–1023. (b) Riggs-Gelasco, P. J.; Price, J. C.; Guyer, R. B.; Brehm, J. H.; Barr, E. W.; Bollinger, J. M., Jr.; Krebs, C. *J. Am. Chem. Soc.* **2004**, *126*, 8108–8109.
- (4) (a) Galonic, D. P.; Barr, E. W.; Walsh, C. T.; Bollinger, J. M., Jr.; Krebs, C. *Nat. Chem. Biol.* **2007**, *3*, 113–116. (b) Hoffart, L. M.; Barr, E. W.; Guyer, R. B.; Bollinger, J. M., Jr.; Krebs, C. *Proc. Natl. Acad. Sci. U.S.A.* **2006**, *103*, 14738–14743.
- (5) Vaillancourt, F. H.; Yeh, E.; Vosburg, D. A.; Garneau-Tsodikova, S.; Walsh, C. T. *Chem. Rev.* **2006**, *106*, 3364–3378.
- (6) Noack, H.; Siegbahn, P. E. M. *J. Biol. Inorg. Chem.* **2007**, *12*, 1151–1162.
- (7) (a) de Visser, S. P. *Angew. Chem., Int. Ed.* **2006**, *45*, 1790–1793. (b) de Visser, S. P. *J. Am. Chem. Soc.* **2006**, *128*, 9813–9824. (c) de Visser, S. P. *Chem. Commun.* **2007**, 171–173. (d) Godfrey, E.; Porro, C. S.; de Visser, S. P. *J. Phys. Chem. A* **2008**, *112*, 2464–2468.
- (8) (a) Becke, A. D. *J. Chem. Phys.* **1993**, *98*, 5648–5652. (b) Lee, C.; Yang, W.; Parr, R. G. *Phys. Rev. B* **1988**, *37*, 785–789. (c) *Jaguar 7.0*; Schrödinger, LLC.: New York, 2007.
- (9) Hay, P. J.; Wadt, W. R. *J. Chem. Phys.* **1985**, *82*, 270–283.
- (10) Shaik, S.; Kumar, D.; de Visser, S. P. *J. Am. Chem. Soc.* **2008**, *130*, 10128–10140.

JP8097632